Bull. ERS, No. 21 (1988)

RESPONSE OBSERVATION OF SCALED MODEL STRUCTURES TO STRONG EARTHQUAKES

Koichi TAKANASHI (I)
Kenichi OHI (II)

SUMMARY

Scaled model structures with intentionally reduced seismic strength to 1/3 to 1/2 were constructed in 1983 for long term observation in order to collect data of earthquake response and grasp failure mechanisms during earthquakes. A monitoring system was installed in the structures as well as in the surrounding soil. Since then, a great deal of date were recorded for many earthquakes [1]. Among them, various kinds of data describing response behavior during four strong earthquakes were successfully collected. These date are examined and compared each other in this paper. Some tentative conclusions are drawn for elastic-plastic behavior, interactions between structures and soil, and soil behavior.

INTRODUCTION

It is well known that complex vibration occurs in structures and their foundation during earthquakes and that this behavior has a great impact on the failures. To obtain the true solution to these problems, there is a pressing need to collect actual data by directly observing ground motions, response of structural systems and their interaction, though the response behavior is to be predicted to some extent by theoretical analyses, by model tests and by analyzing damages due to earthquake disasters.

The collected data are useful for analyses of the actual behavior of soils and structures. In addition, the data are very effective in verifying and developing theoretical analyses. From this point of view, Institute of Industrial Science set out a project for research on the response and failure mechanism of a ground-structure system under real earthquakes. This research project is mostly conducted at the Chiba Experiment Station of Institute of Industrial Science, 31 km east of Tokyo. This research includes the earthquake response observation of structures with

---

(I) Professor, Institute of Industrial Science, University of Tokyo, TOKYO, JAPAN
(II) Lecturer, Institute of Industrial Science, University of Tokyo, TOKYO, JAPAN

intentionally reduced the seismic strength which may be damaged even by moderate earthquakes. There are a lot of response data to a number of earthquakes obtained already since 1983. Most of such earthquakes are "small", but a few should be called "strong". Among them, the shock on October 4, 1985, which was announced the strongest in past 56 years in Tokyo, the another shock on December 17, 1987 were classified to "strong" earthquake. Its intensity was assigned to the grade V of JMA Scale.

In this paper the observation records of two steel structures are presented. These records were obtained during four stronger earthquakes including the above two strong earthquakes. The location of the observation site and epicenters of the earthquakes are shown in Fig.1. Dates of occurrences, magnitudes and epicenters of these earthquakes are summarized in Table 1.

STRUCTURE MODELS AND INSTRUMENTATION

The two structural steel models were constructed on the actual ground as shown in Fig.2. Each model is described as follows:

(1) Model No.1

A three-story moment resistant frame composed of H-shaped columns (H-125x 125x6.5x9) and H-shaped girders; x and y directions shown in Fig.2 coincide with the weak axis and the strong axis of the H-shaped column section, respectively.

(2) Model No.2

A three-story braced frame composed of H-shaped columns (H-150x50x5x7), H-shaped girders and braces; the braces in the x-direction are composed of rectangular section (plate 6x10x400) in a part, connected to angles (L-65x65x6) and the braces in the y-direction are composed of angle members (L-65x65x6). The braces in the y-direction are installed for preventing catastrophic collapse due to twisted movements after buckling of the braces in the x-direction which causes the unbalance in horizontal rigidity. The braces of the rectangular section were immediately replaced by the new after the buckling failure due to the past strong earthquakes. The yield base shear force of the x-direction is 9% of total building weights, and this strength is less than one-third of the design practice in Japan.

The reinforced concrete base floors (5 meters square) were constructed directly on the surface of the Kanto loam after the top soil was removed. The shapes and the dimensions of the two models are shown in Figs. 3 and 4, and the fundamental parameters are summarized on Tables 2 and 3.

Various types of transducers were installed on the models to measure the following data:

1) Accelerations of each floor, 3x3 components per model.
2) Accelerations of basement, 3 components per model.
3) Inter-story displacements as well as rotation, 4x3 components per model.
4) Flexural strains of the 1st story columns and the axial strains of the braces, 32 components per model.

Additionally the underground accelerations at the depths of 1 meter, 10 meters, 20 meters and 40 meters are recorded simultaneously. The data acquisition is automatically started once 10 mm/s/s is sensed at the depth of 40 meters, and the data are converted into the digital form every sample time of 5 milliseconds.

SUMMARY OF OBSERVED RESPONSE

Response behavior observed during the four earthquakes are summarized in Table 4. In the table peak values of accelerations are primarily shown, which were recorded in the soil 10m and 1m below the ground surface as well as in the model structures. The maximum values of story shears calculated from the recorded accelerations and corresponding story shear coefficients (the story shears divided by the sum of the sustaing upper floor weights) are then presented. Sideway drifts of floors are shown in the same way.

Accelerations of the ground motions

From the observed records of the ground accelerations, the shocks except on December 17, 1987 were assigned to the grade IV of JMA Scale. The shock on December 17, 1987 should be recognized as a grade V earthquake, even though such a classification way from acceleration values are not officially carried out. The other two earthquakes remain in the grade III. Considerable magnification of acceleration is induced in the soil within 10m in depth. As discussed later, the soil retains elastic behavior without any damage.

Responses of model structures

The acceleration values recorded on the base floors are almost same as those recorded in the soil 1m below the ground surface. That means the base floors behaved in the same manners as the ground surface. This evidence will discussed in detail later.

Magnification of acceleration is also observed in the model structures. In the model No.2, however, accelerations in the x-direction of the upper stories didn't become large after buckling failure occurred in the first story. Thus, the damage was concentrated into the first story, as often observed in structural damages in real structures due to strong earthquakes. Such a inelastic behavior of the model No.2 will be discussed later. Response values of the model No.1 remain within elastic ranges.

INELASTIC BEHAVIOR OF BRACED FRAME

In the x-direction of the model No.2 the braces in the first story were buckled and underwent considerable yielding. The story shear vs. drift relationships and their time histories for four earthquakes are shown in Figs.5 to 8. These braces have been replaced by the new immediately after the buckling and yielding failures were found due to the past earthquakes.

Hysteretic behavior

It was commonly observed throughout these figures that buckling of the braces occurred after several reversals of the forces in the elastic range and the maximum value of the first story shear was attained (denoted by A in each figure a). It was followed by considerable story drifts. Finally these loops were merged into small loops with much smaller stiffness than the initial.

Differences exist not only in the amounts of the drifts, but also in the hysteretic behavior in Figs.5 to 8. These were caused by both the intensity and the frequency characteristics of each earthquake.

The braces in the y-direction of the model No.2 were installed to prevent a complete failure due to twisting vibrations. Therefore these were proportioned according to the practical design rule. The story shear vs. drift relationship and their time histories for December 17 earthquake are shown in Fig.9. Apparently the braces underwent yielding because hysteresis loops are observed. These were caused by the yielding at the joint parts where the braces are connected to gausset plates by high strength bolts. The current design rule should be considered to be reasonable.

Maximum Load-Carrying Capacity

The maximum load-carrying capacity Pmax (point A) can be evaluated by the sum of the strength of braces and frames:

$$P_{max} = n(\sigma_y A_e + \sigma_{cr} A_e) + (k_c - k_d)\, d_0$$

where
σ_{cr}: Euler's buckling stress
σ_y : yield stress
A_e : sectional area of brace
n : numbers of pairs of bars
k_c : elastic stiffness of columns
k_d : stiffness reduction due to PΔ effect
d_0 : observed drift at maximum story shear force

In the evaluation of the buckling stress, it is assumed that the effective buckling length is 60 % of the clear length. Calculated Euler's buckling stress is about 98 MPa. In the evaluation of the yield stress, the strain-rate effects on yields stress should be considered. As is often experienced, under the higher strain rate the yield stress slightly increases. The duration of yielding from the point A to the unloading point B shown in Fig.5 is very short time of 0.1 seconds, and the averaged strain rate reaches 0.12 per second. Then, a higher value, 343 MPa, should be assigned to the yield stress. The evaluated load-carrying capacity is also marked in Figs.5 to 8.

SPECTRAL ANALYSES AND NATURAL FREQUENCIES

The FFT techniques are utilized in order to identify the spectral characteristics of the soil-structure interaction systems. The data processing in the system identification was carried out in the following way [2)]:

(1) Consider the unknown system, whose input and output time series are denoted by x(t) and y(t), respectively. The Foureir transforms of these time series, $X(\omega)$ and $Y(\omega)$, can be approximated by the finite complex Fourier components in the FFT computation. The data length used is 40.96 seconds and the data size is 8192.

(2) The energy spectrum or the Fourier square amplitude spectrum of the input time series, denoted by Sxx, and the cross spectrum of the input and output time series, denoted by Sxy, are calculated under the following definitions:

$$Sxx = X^*(\omega)\, X(\omega) \tag{2}$$

$$Sxy = X^*(\omega)\, Y(\omega) \tag{3}$$

where $X^*(\omega)$ denotes the conjugate of $X(\omega)$.

Evidently Sxx and Sxy indicate the contribution of each spectral component

to the two integrals $\int (x(t))^2\, dt$ and $\int x(t)y(t)\, dt$, respectively.
(3) The FFT techniques have high resolving capacity, but the computed spectral values often shows abrupt changes, which may be caused by some errors included in the data. In order to remove these unstable changes and to pay attention to slowly changed essentials, some smoothing techniques are applied to the spectral values. In this paper, the computed spectral values, Sxx and Sxy, are smoothed by a rectangular spectral window, the band width of which is set to 0.3 Hz. This smoothing process makes no change in the original values of the two integrals $\int (x(t))^2\, dt$ and $\int x(t)y(t)\, dt$. The smoothed energy spectrum and the smoothed cross spectrum are denoted by $\overline{Sxx}$ and $\overline{Sxy}$, respectively.
(4) The system function of this input-output system, denoted by $H(\omega)$, is defined as a complex function, which satisfies the following equation:

$$Y(\omega) = H(\omega)\ X(\omega) \tag{4}$$

The system function $H(\omega)$ can be identified by:

$$H(\omega) = \overline{Sxy}\ /\ \overline{Sxx} \tag{5}$$

Four observed acceleration records, which are recorded at 1) 40m deep in the soil, 2) 1m deep, 3) the basement, 4) the roof for each earthquake are chosen to identify three kinds of input-output systems, from 1) to 2), from 2) to 3) and from 3) to 4). The smoothed Fourier amplitude spectra of the above four records and the three system gains are shown in Figs.10 to 21 for each directions of the two models. The square root values of the smoothed energy spectra are plotted as the smoothed Fourier amplitude spectra, and absolute values of system functions identified by Eq. 5 are plotted as the system gains.

Soil Condition

There exists a thick layer of Kanto loam under a thin surface layer at the site of the observation. The soil condition should be classified into the grade suitable for structural construction. In the system gains of the soil between 40m and 1m below the surface, three peaks at 2 Hz, 5.5 ∿ 6.0 Hz and 8.5 Hz are commonly observed for four earthquakes. It shows the characteristics of the soil and also the soil still remains in the elastic condition without yielding.

Interaction between Soil and Structures

The system gain obtained from the records in the soil 1m below the surface and on the base floor shows that the gains for the frequencies less than 5Hz can be regarded as almost unit except those in the y-direction of the model No.2. It can be concluded that the base floor moved in the same manner as the soil near the surface at least for the movements with frequency components less than 5 Hz. As for the gains in the y-direction of the model No.2, the gain of 4.5 Hz is dominant in the cases of three earthquakes except December 17 earthquake. This frequency coincides with the dominant frequency of the model structure. This fact shows the existence of rocking movements. It was caused by a rigid motion of the structure which is provided with a high stiffness of strong braces. This explanation can also be adopted for the absense of a rocking movement during December 17 earthquake, where the braces were yielded to decrease their stiffness.

CONCLUDING REMARKS

(1) An outline of the elastic and inelastic responses due to four strong earthquakes have been described. The data acquisition system works well, and especially, inelastic responses of steel structure accompanied by buckling and yielding of the braces have been successfully recorded.

(2) System identification techniques using Fast Fourier Transform are applied to the observed acceleration records. Identified system gains from the underground of 1m deep to the base floors are found to be low-pass filters.

(3) The model No.2 was damaged for all four earthquakes. The damaged behavior can be predicted if the strain rate effect on the yield stress of the steel material is considered and the ground excitation at the site is precisely evaluated.

ACKNOWLEDGEMENTS

The writers would like to express their appreciation to Mr. Y. Shimawaki and Mr. H. Kondo, technical officials of Institute of Industrial Science, University of Tokyo, for their supports during this study.

REFERENCES

1. Bulletin of ERS, Earthquake Resistant Structure Research Center, Institute of Industrial Science, University of Tokyo, No.19, March 1986.
2. Hino, M., Spectral Analysis, ASAKURA-SHOTEN Co., Inc. Oct. 1977 (in Japanese)

Table 1 Earthquakes

	Date	N.Lat.	E.Long.	Depth	Magnitude
1)	1985 10/04 21:26	$34^\circ 53'$	$140^\circ 09'$	78km	6.2
2)	1985 11/06 00:31	$35^\circ 22'$	$140^\circ 14'$	59km	5.1
3)	1986 06/24 11:53	$34^\circ 08'$	$140^\circ 08'$	80km	6.9
4)	1987 12/17 11:08	$35^\circ 21'$	$140^\circ 29'$	58km	6.7

Table 2 Parameters of model No.1

Stories	3
Area of each floor	25.1 m^2
Weigth of each floor	124 KN
Steel grade	JIS SS41
Steel members	C1:H-125x125x6.5x9 G1:H-200x100x5.5x8 Brace:L-65x65x6

Table 3 Parameters of model No.2

Stories	3
Area of each floor	25.1 m^2
Weigth of each floor	172 KN
Steel grade	JIS SS41
Steel members	C2:H-125x125x6.5x9 G2:H-200x100x5.5x8 Brace:PL-6x10

Table 4 Peak values of response observed

(a) October 4, 1985

model		No.1		No.2	
direction		x (weak)	y (strong)	x (weak)	y (strong)
	-40m	200	180	190	200
	-20m	290	210	250	250
	-10m	360	300	330	330
acc.	-1m	880	770	840	860
(mm/	Base Fl.	860	630	710	730
sec)	2 Fl.	1640	1380	1710	1330
	3 Fl.	1310	1280	880	2590
	R Fl.	1800	1390	1650	3520
story*	1st st.	31.7(0.08)	36.3(0.09)	69.4(0.13)	23.8(0.04)
shear	2nd st.	29.2(0.10)	24.8(0.09)	68.4(0.20)	18.0(0.05)
(KN)	3rd st.	24.2(0.18)	18.7(0.14)	45.6(0.27)	10.8(0.06)
story	1st st.	12.0	5.6	4.6	1.2
drift	2nd st.	11.1	4.0	1.1	0.8
(mm)	3rd st.	8.8	2.8	0.6	0.4

* Values in parentheses indicate story shear coefficients

(b) November 6, 1985

model		No.1		No.2	
direction		x (weak)	y (strong)	x (weak)	y (strong)
acc. (mm/sec)	-40m	180	150	150	200
	-20m	200	240	260	220
	-10m	300	320	330	320
	-1m	810	720	810	740
	Base Fl.	810	740	710	590
	2 Fl.	500	880	1550	1030
	3 Fl.	440	810	1360	1860
	R Fl.	430	1020	1840	2460
story* shear (KN)	1st st.	5.5(0.01)	19.3(0.05)	53.5(0.10)	24.5(0.05)
	2nd st.	5.1(0.02)	14.2(0.05)	51.2(0.15)	18.5(0.05)
	3rd st.	5.8(0.04)	13.7(0.10)	32.8(0.19)	9.7(0.06)
story drift (mm)	1st st.	2.0	3.0	2.9	0.8
	2nd st.	1.9	2.2	1.2	0.5
	3rd st.	2.0	2.0	0.6	0.2

* Values in parentheses indicate story shear coefficients

(c) June 24, 1986

model		No.1		No.2	
direction		x (weak)	y (strong)	x (weak)	y (strong)
acc. (mm/sec)	-40m	140	150	160	120
	-20m	190	220	250	160
	-10m	220	280	320	190
	-1m	530	630	660	490
	Base Fl.	380	780	760	540
	2 Fl.	1230	1310	1680	1320
	3 Fl.	950	1170	1400	2480
	R Fl.	1050	1620	1850	3400
story shear (KN)	1st st.	22.5(0.06)	30.4(0.08)	69.6(0.13)	24.1(0.05)
	2nd st.	17.9(0.07)	24.4(0.09)	67.3(0.19)	18.8(0.05)
	3rd st.	14.3(0.11)	21.9(0.17)	43.6(0.25)	10.1(0.06)
story drift (mm)	1st st.	8.4	4.7	6.1	1.2
	2nd st.	6.5	6.5	1.0	0.8
	3rd st.	5.0	5.0	0.6	0.4

* Values in parentheses indicate story shear coefficients

(d) December 17, 1987

model		No.1		No.2	
direction		x (weak)	y (strong)	x (weak)	y (strong)
acc. (mm/sec)	-40m	950	920	810	960
	-20m	900	1050	1060	950
	-10m	1310	1210	1180	1260
	-1m	2800	3300	2830	3330
	Base Fl.	2820	3200	2840	3010
	2 Fl.	3010	6480	1840	4200
	3 Fl.	2530	6460	1670	5210
	R Fl.	2960	6500	1980	7410
story shear (KN)	1st st.	47.5(0.12)	128.6(0.32)	166.5(0.32)	114.4(0.22)
	2nd st.	37.1(0.14)	96.8(0.37)	158.5(0.45)	91.9(0.26)
	3rd st.	39.9(0.30)	87.8(0.67)	96.8(0.56)	46.7(0.26)
story drift (mm)	1st st.	18.5	20.7	20.6	6.5
	2nd st.	14.6	16.7	1.7	2.4
	3rd st.	15.5	13.5	0.7	1.0

* Values in parentheses indicate story shear coefficients

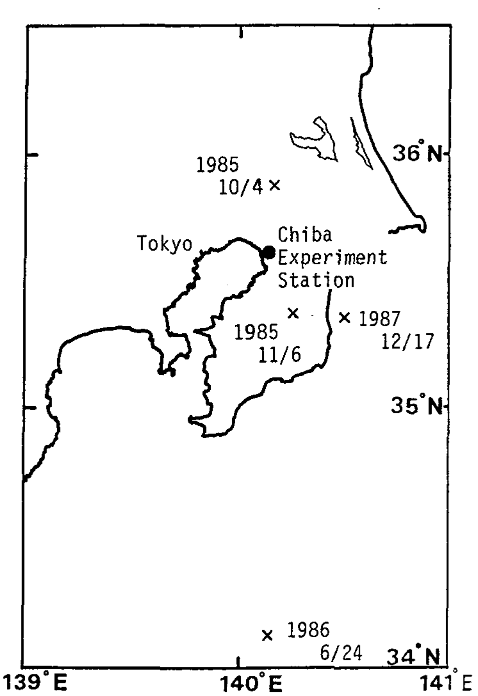

Fig. 1 Dates and Epicenters of Earthquakes

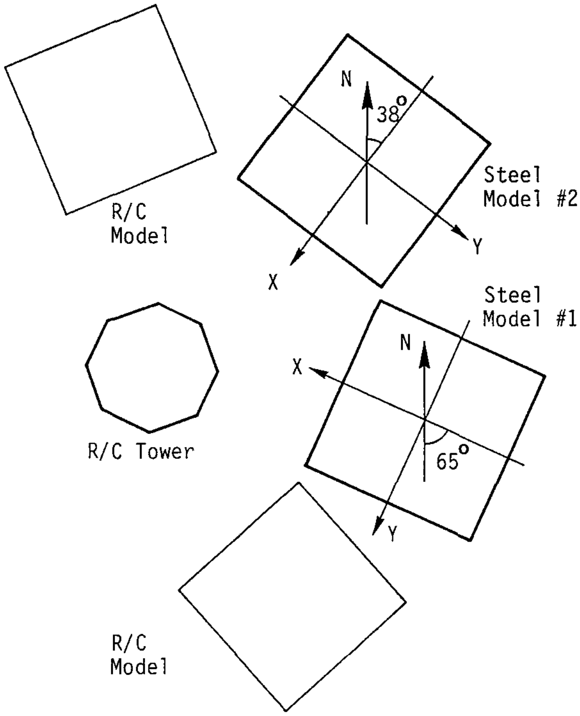

Fig. 2 Model Locations at Observation Site

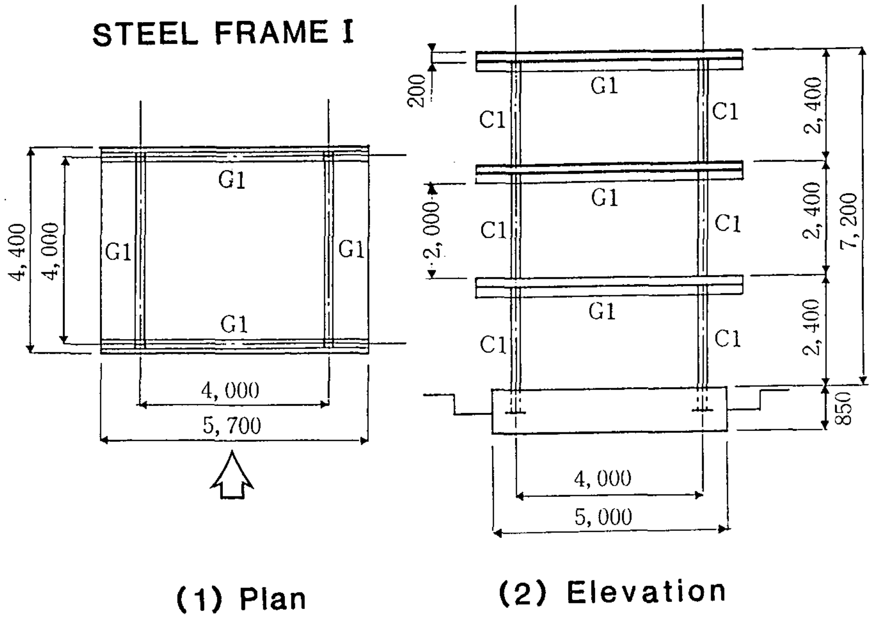

Fig. 3 Framework and Dimensions of Model No.1

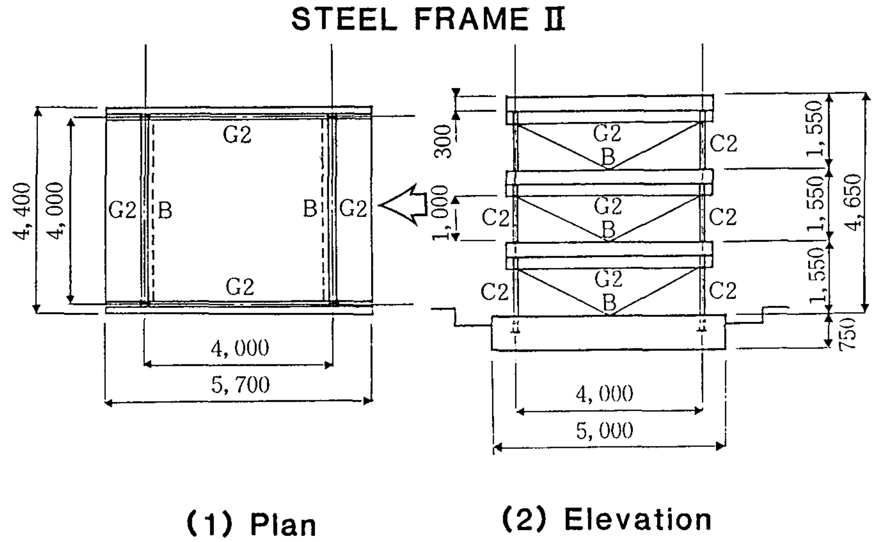

Fig. 4 Framework and Dimensions of Model No.2

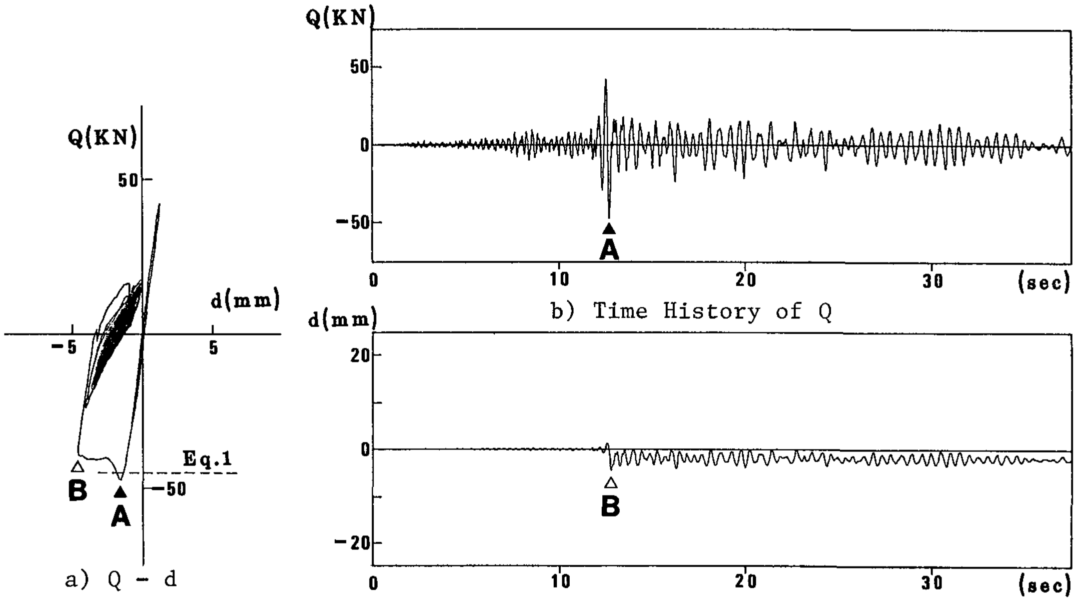

a) Q - d

b) Time History of Q

c) Time History of d

Fig. 5 Response to 10/4 Earthquake

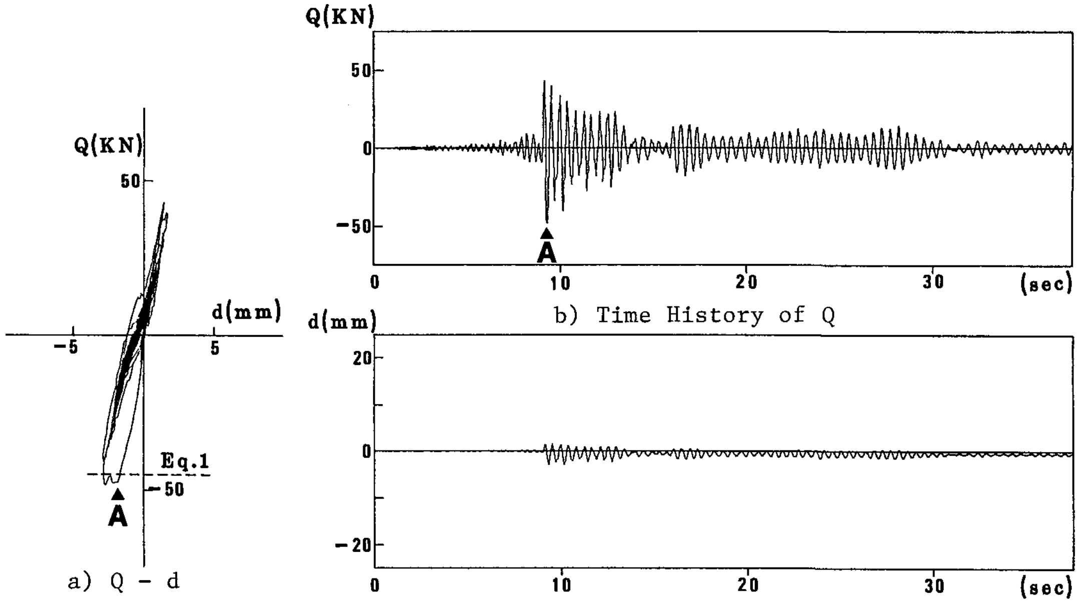

a) Q - d

b) Time History of Q

c) Time History of d

Fig. 6 Response to 11/6 Earthquake

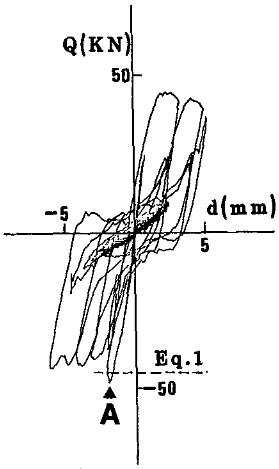

a) Q - d

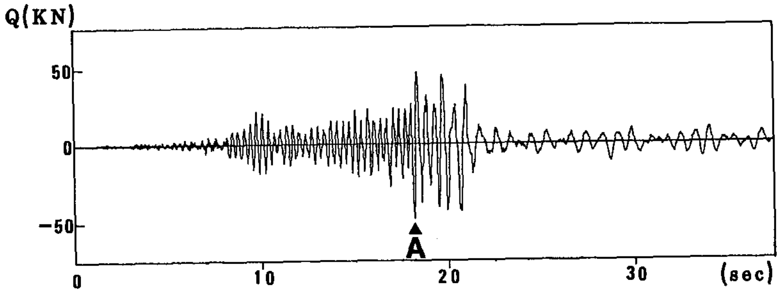

b) Time History of Q

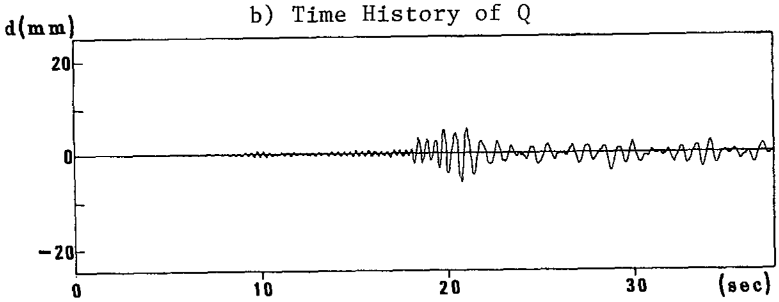

c) Time History of d

Fig. 7 Response to 6/24 Earthquake

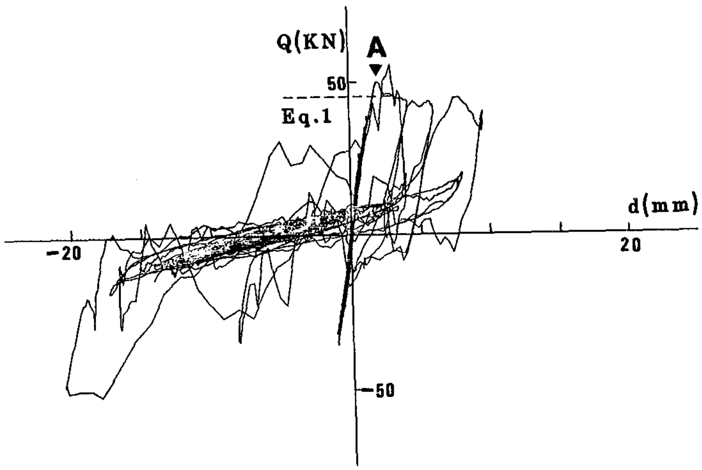

a) Q - d

Fig. 8 Response to 12/17 Earthquake (x-direction)
(to be cont'd)

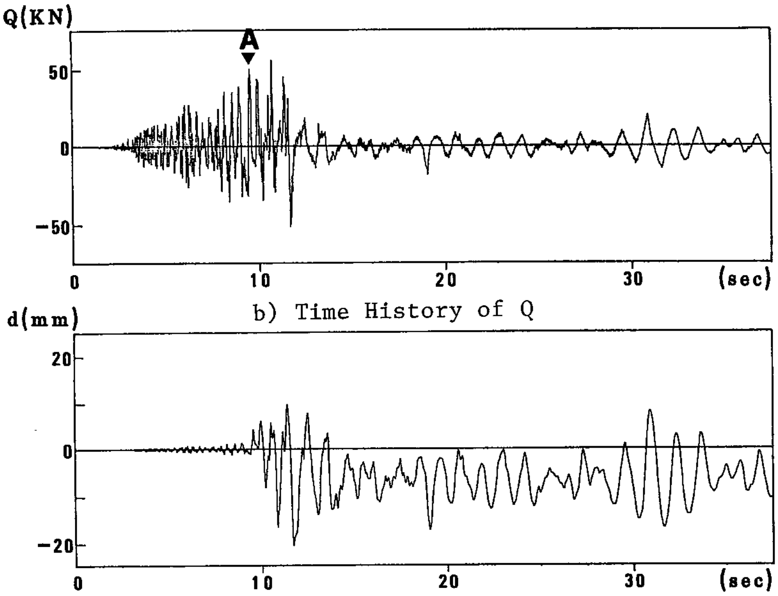

b) Time History of Q

c) Time History of d

Fig. 8 Response to 12/17 Earthquake (x-direction)

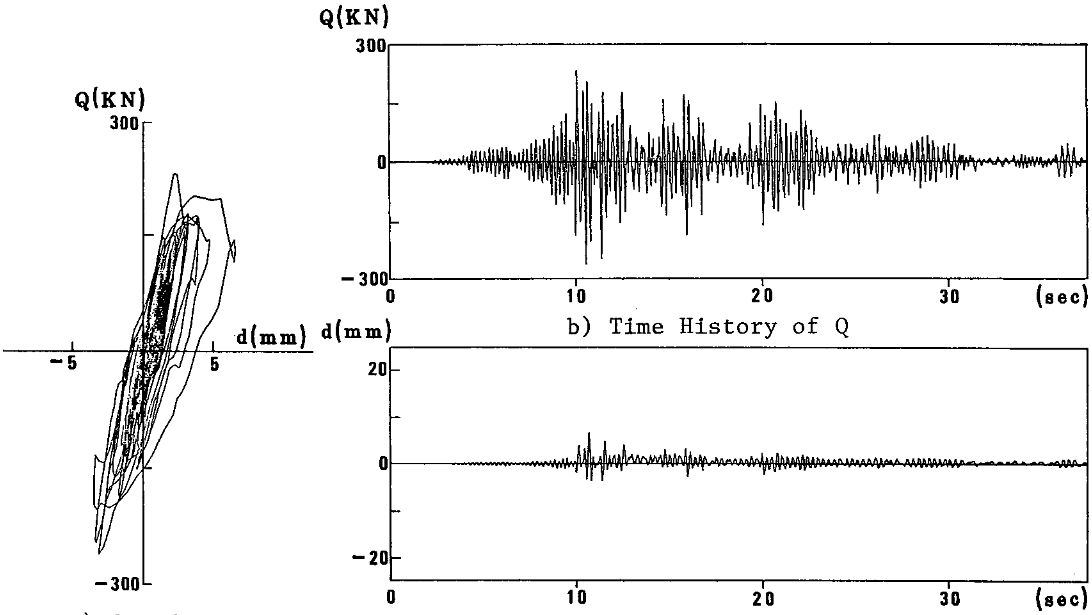

a) Q - d

b) Time History of Q

c) Time History of d

Fig. 9 Response to 12/17 Earthquake (y-direction)

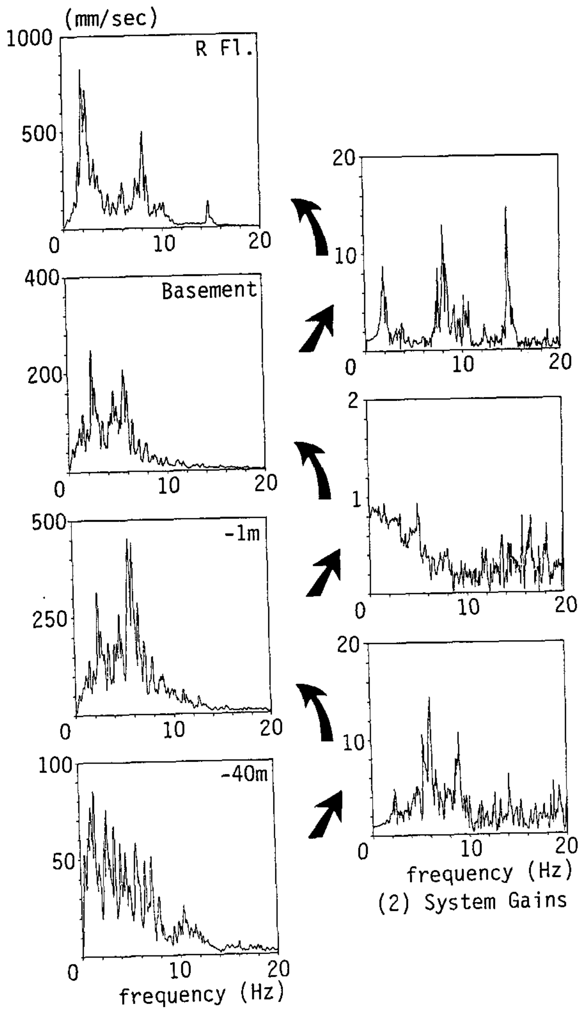

(1) Fourier spectra

Fig. 10 Fourier Spectra and System Gains at Oct. 4, 1985 (Model No.2, X-direction)

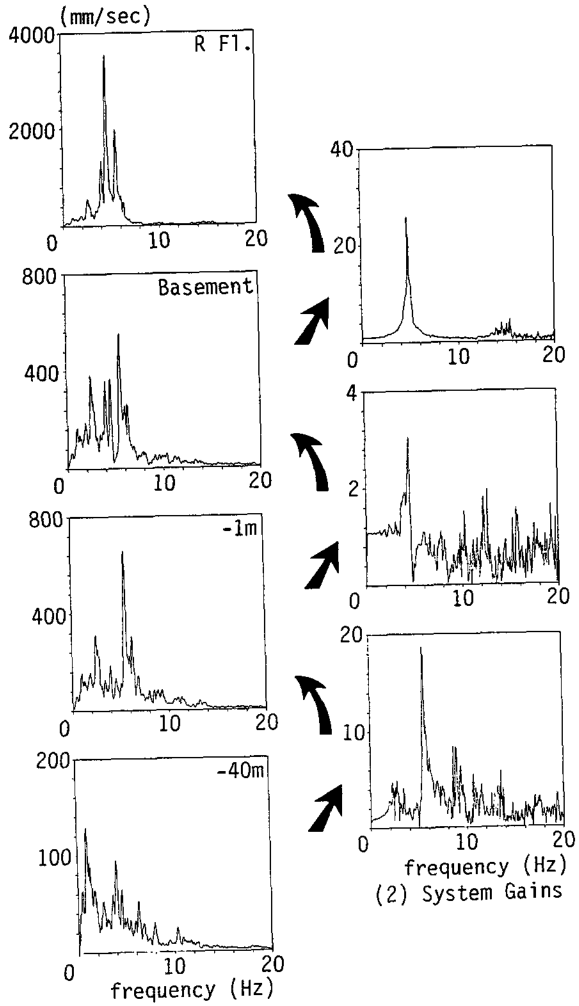

(1) Fourier spectra

Fig. 11 Fourier Spectra and System Gains at Oct. 4, 1985 (Model No.2, y-direction)

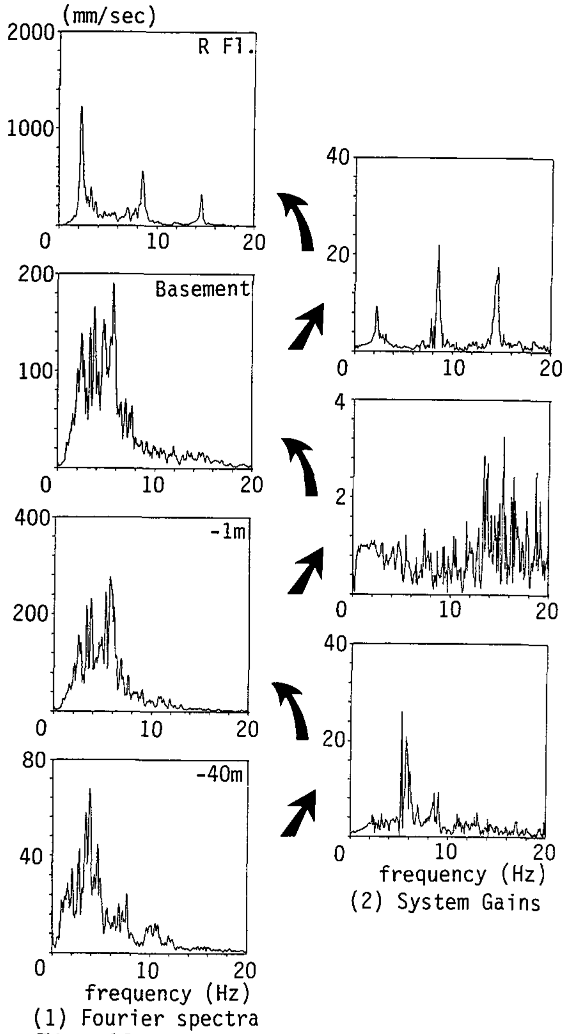

Fig. 12 Fourier Spectra and System Gains at Nov. 6, 1987 (Model No.2, X-direction)

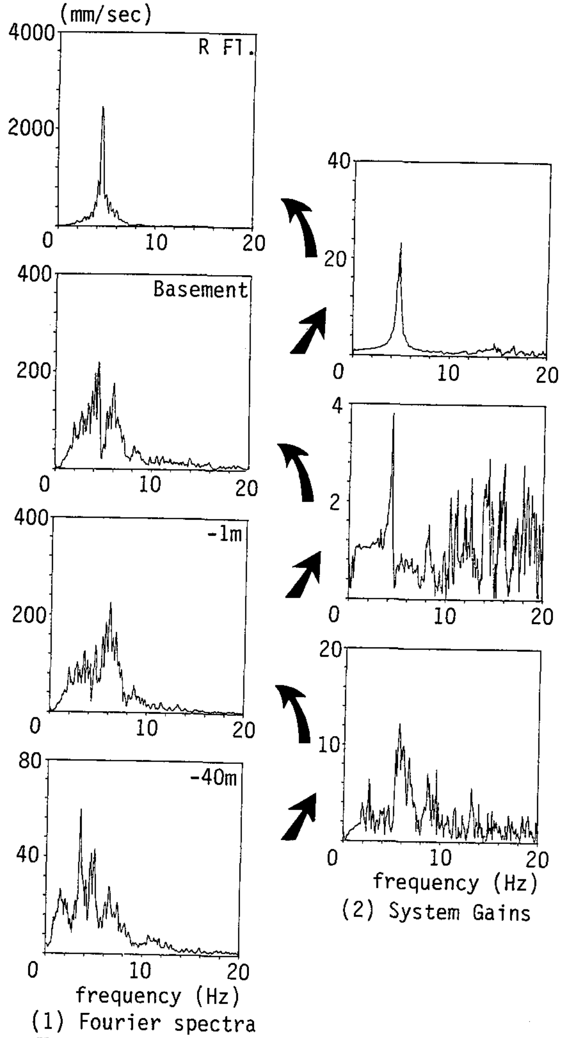

Fig. 13 Fourier Spectra and System Gains at Nov. 6, 1987 (Model No.2, y-direction)

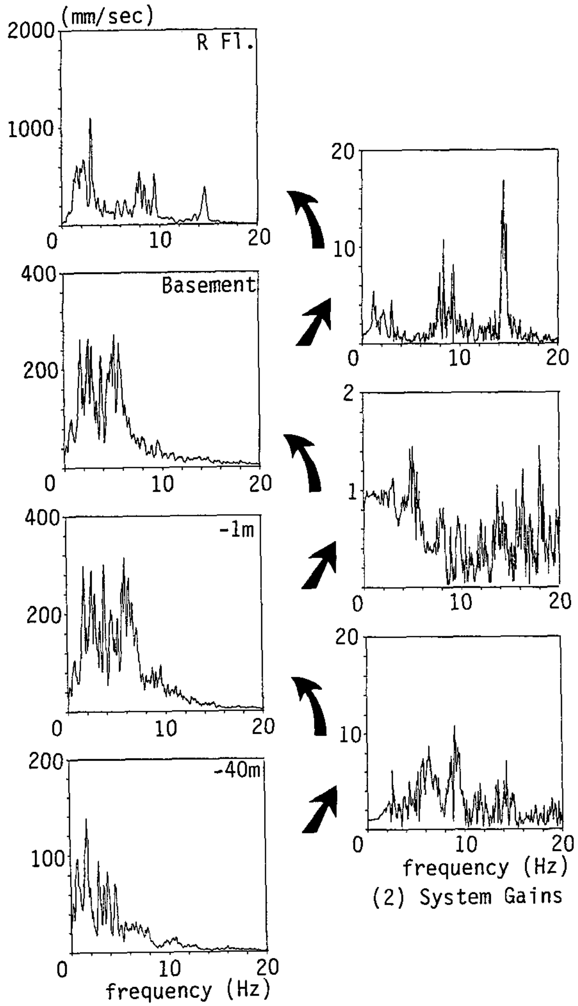

(1) Fourier spectra

Fig. 14 Fourier Spectra and System Gains at June. 24, 1985 (Model No.2, X-direction)

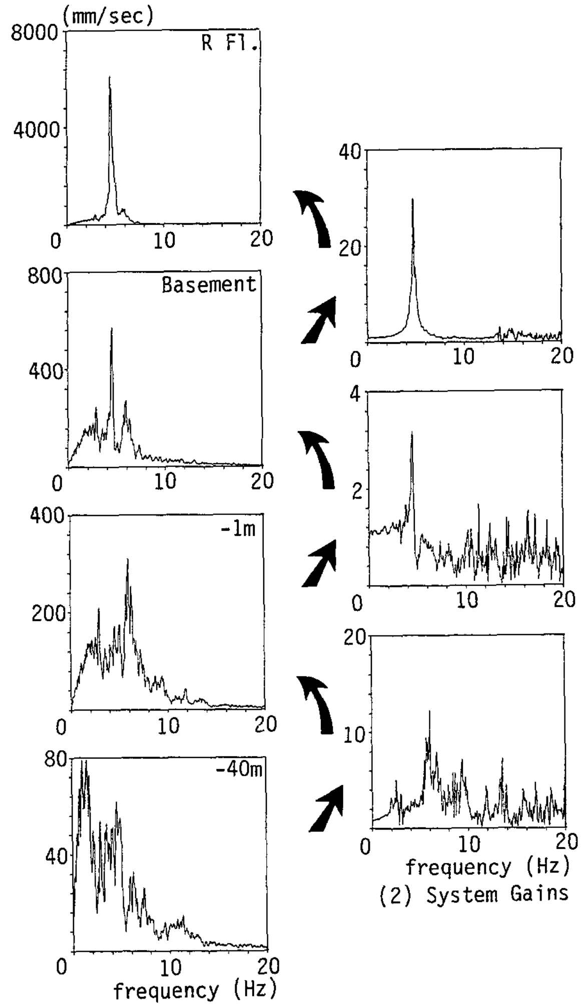

(1) Fourier spectra

Fig. 15 Fourier Spectra and System Gains at June. 24, 1985 (Model No.2, y-direction)

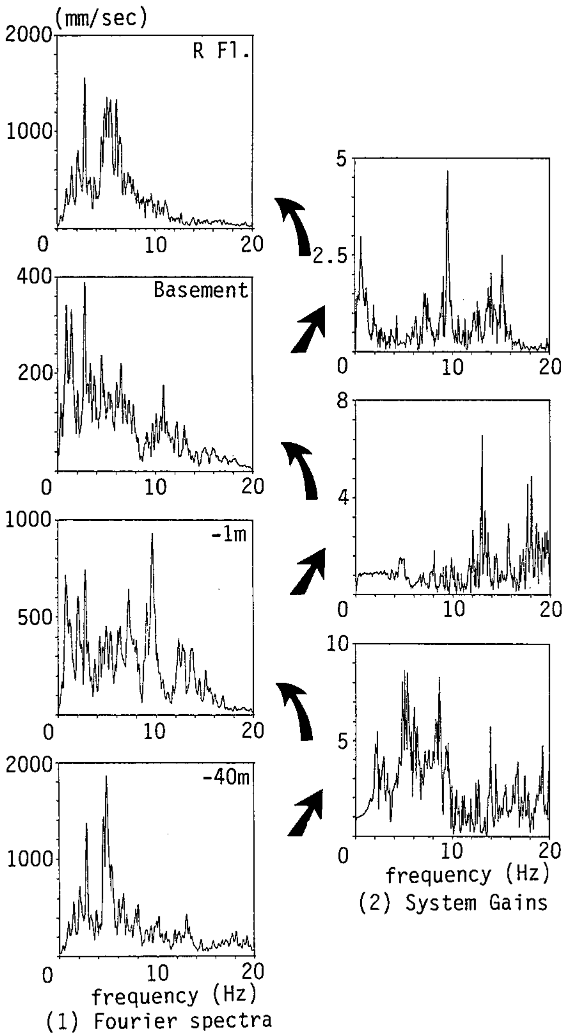

Fig. 16 Fourier Spectra and System Gains at Dec. 17, 1987 (Model No.2, X-direction)

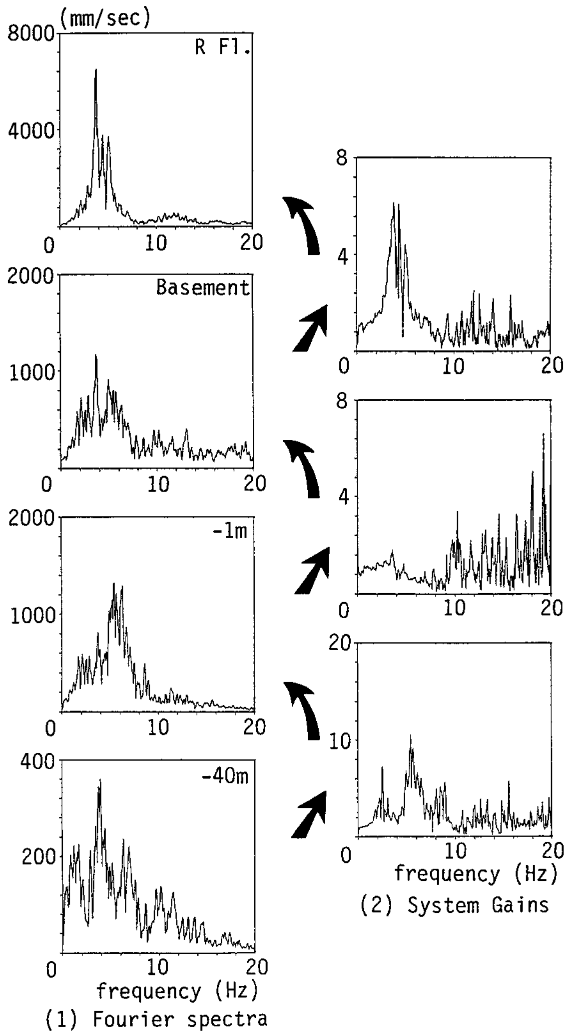

Fig. 17 Fourier Spectra and System Gains at Dec. 17, 1987 (Model No.2, y-direction)

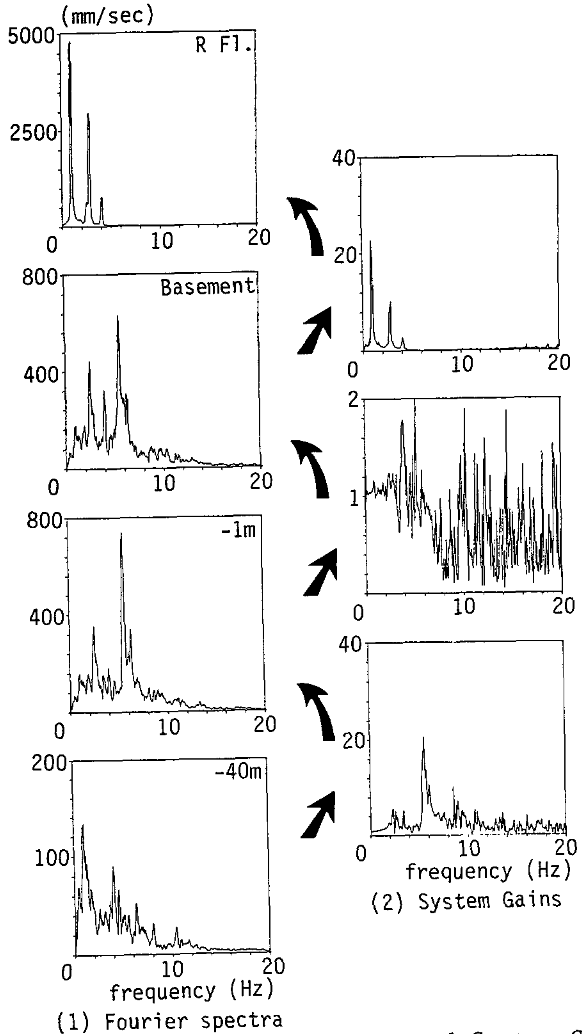

Fig. 18 Fourier Spectra and System Gains at Oct. 4, 1985 (Model No.1, X-direction)

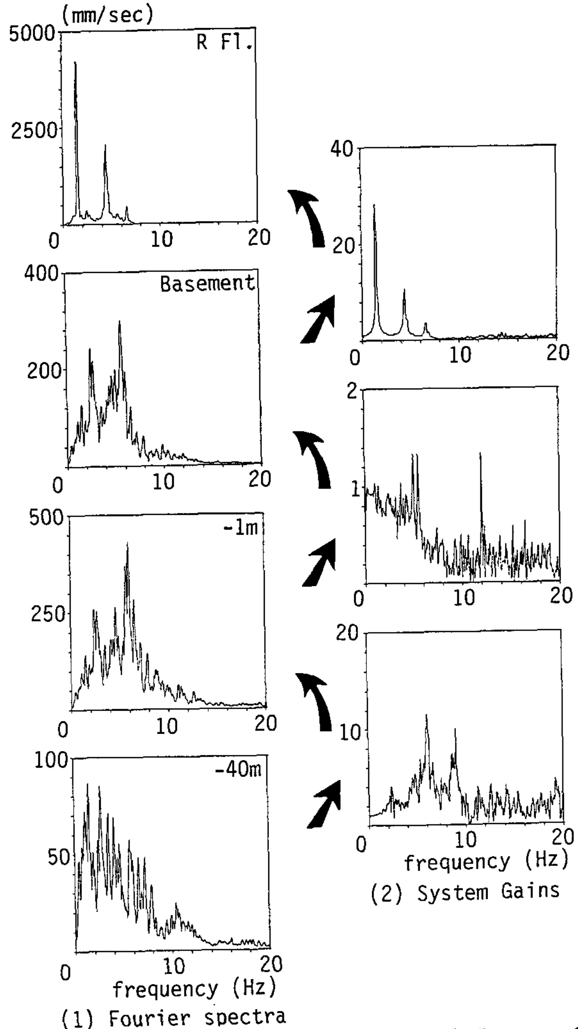

Fig. 19 Fourier Spectra and System Gains at Oct. 4, 1985 (Model No.1, y-direction)

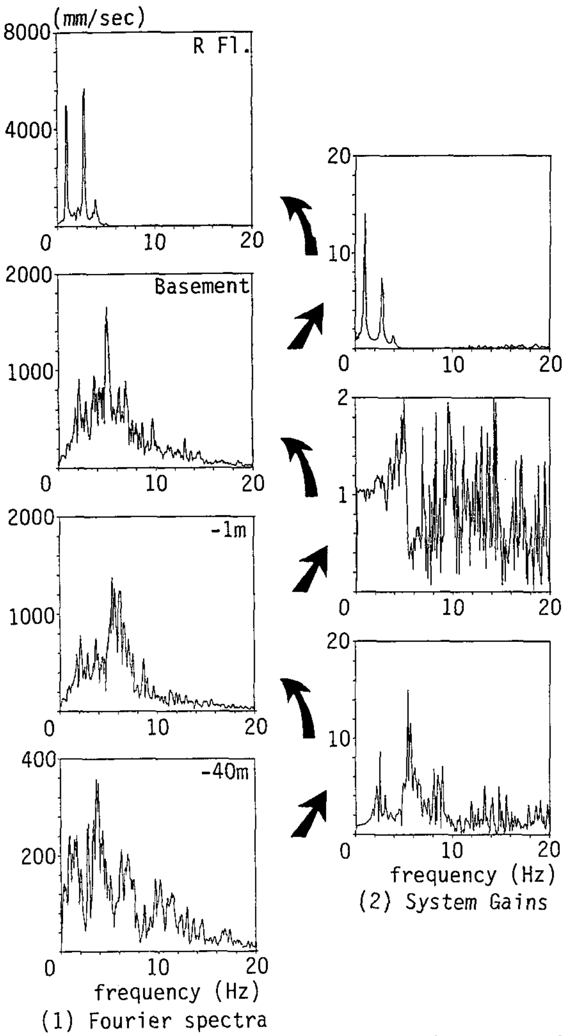

Fig. 20 Fourier Spectra and System Gains at Dec. 17, 1987 (Model No.1, X-direction)

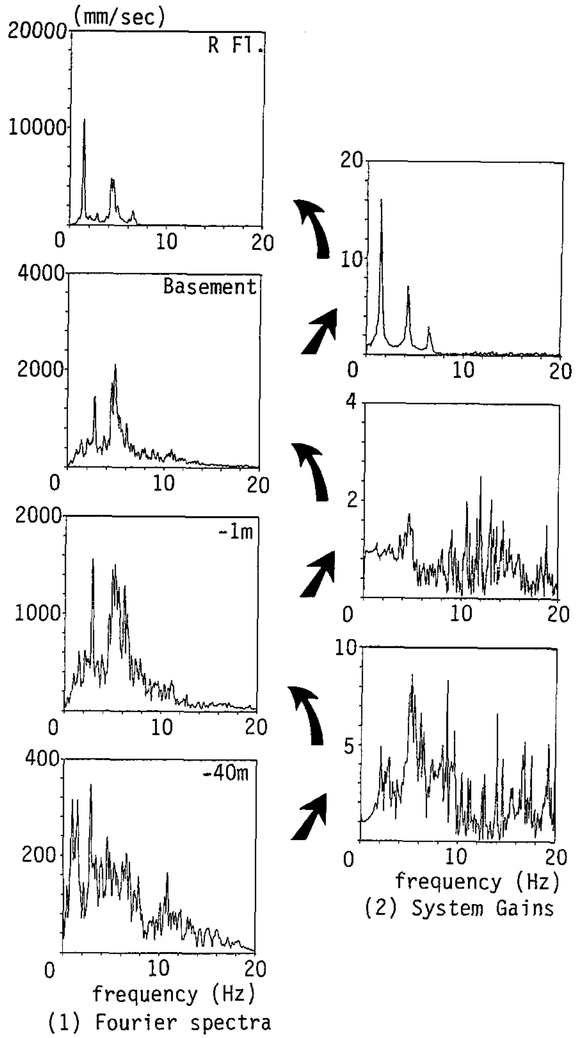

Fig. 21 Fourier Spectra and System Gains at Dec. 17, 1987 (Model No.1, y-direction)